Faceted phospholipid vesicles tailored for the delivery of *Santolina insularis* essential oil to the skin

Ines Castangia,[a] Maria Letizia Manca,[a] Carla Caddeo,[a,*] Andrea Maxia,[b] Sergio Murgia,[c] Ramon Pons,[d] Davide Demurtas,[e] Daniel Pando,[f] Danilo Falconieri,[b] José E. Peris,[g] Anna Maria Fadda,[a] Maria Manconi[a]

[a] Dept. Scienze della Vita e dell'Ambiente, Drug Science Division, University of Cagliari, 09124 Cagliari, Italy
[b] Dept. Scienze della Vita e dell'Ambiente, Botany and Botanical Garden Division, University of Cagliari, 09124 Cagliari, Italy
[c] Dept. Scienze Chimiche e Geologiche, CNBS and CSGI, University of Cagliari, Monserrato (CA), Italy
[d] Dept. Tecnologia Química i de Tensioactius, Institut de Química Avançada de Catalunya (IQAC-CSIC) 08034 Barcelona, Spain
[e] Interdisciplinary Center for Electron Microscopy, Ecole Polytechnique Fédérale de Lausanne, Station 12, 1015-Lausanne, Switzerland
[f] Dept. Ingeniería Química y Tecnología del Medio Ambiente, University of Oviedo, Oviedo, Spain
[g] Dept. Farmacia y Tecnologia Farmaceutica, University of Valencia, 46100-Burjassot, Valencia, Spain

*Corresponding author: Carla Caddeo

Dept. Scienze della Vita e dell'Ambiente, Drug Science Division, University of Cagliari, 09124 Cagliari, Italy

Tel.: +39 0706758582; fax: +39 0706758553; e-mail address: caddeoc@unica.it

ABSTRACT

The aim of this work was to formulate *Santolina insularis* essential oil-loaded nanocarriers, namely Penetration Enhancer containing Vesicles (PEVs), evaluate the physico-chemical features and stability, and gain insights into their ability to deliver the oil to the skin.

Santolina insularis essential oil was obtained by steam distillation, and was predominantly composed of terpenes, the most abundant being β-phellandrene (22.6%), myrcene (11.4%) and curcumenes (12.1%). Vesicles were prepared using phosphatidylcholine, and ethylene or

propylene glycol were added to the water phase (10% v/v) to improve vesicle performances as delivery systems. Vesicles were deeply characterized by light scattering, cryogenic transmission electron microscopy and small/wide-angle X-ray scattering, the results showing polyhedral, faceted, unilamellar vesicles of ~115 nm in size. The presence of the glycols improved vesicle stability under accelerated ageing conditions, without changes in size or migration phenomena (e.g., sedimentation and creaming). Confocal laser scanning microscopy images of pig skin treated with *Santolina insularis* formulations displayed a penetration ability of PEVs greater than that of control liposomes. Moreover, all formulations showed a marked in vitro biocompatibility in human keratinocytes.

These findings suggest that the nanoformulation may be of value in enhancing the delivery of *Santolina insularis* essential oil to the skin, where it can exert its biological activities.

Keywords: *Santolina insularis* essential oil; terpenes; phospholipid vesicles; ethylene/propylene glycol; human keratinocytes; pig skin.

1. Introduction

The development of safe and atoxic antibacterial compounds is becoming critical in several fields, such as alimentary, cosmetic and pharmaceutical. To this purpose, plant extracts or essential oils are being widely proposed as sources of natural antimicrobial compounds [1,2]. Essential oils are odorous, volatile products of the secondary metabolism of aromatic plants, and many of them have been reported to possess strong antibacterial, antifungal and antiviral properties [3–5]. In recent years, essential oils have been studied and used as sources of natural antimicrobic agents for the storage stability of foods and industrial products, as well as to treat human pathologies as an alternative to synthetic drugs [6–8]. Additionally, essential oils are rich in terpenoids, which represent a natural defence against oxidative stress, by suppressing nuclear factor-κβ signaling, an important regulator factor of inflammatory diseases and cancer [9]. Thanks to these properties, essential oils are widely used in pharmaceutical and cosmetic preparations as active ingredients or fragrances.

Santolina insularis (Gennari ex Fiori) Arrigoni is an endemic species of Sardinia island (Italy), belonging to Asteraceae family, mainly distributed on mount Gennargentu (central Sardinia) and Marganai-Linas massifs (south-west Sardinia). It is known in Sardinian folk medicine for its anthelmintic properties. In previous works, *Santolina insularis* essential oil was isolated and characterized, and its antibacterial and antiviral properties were studied [10–12].

Despite the promising properties, the high volatility and low water solubility can affect the efficacy of essential oils. Micro- and nanoencapsulation may represent an ideal approach to increase the persistence and efficacy of bioactive essential oils by reducing their volatility and degradation, and improving their bioavailability at the target site [13]. In a previous work, the antiherpetic activity of *Santolina insularis* essential oil was enhanced by its nanoentrapment in liposomes [12]. Liposomes and liposome-like vesicles play an important role in drug

delivery for their properties and versatility [14,15]. In skin delivery, liposomes are considered more useful for the local deposition of drugs, while innovative modified phospholipid vesicles (e.g., ethosomes, transfersomes, invasomes and PEVs-Penetration Enhancer containing Vesicles) have been designed to actively deliver the drug to the deeper skin layers, or even to the systemic circulation.

Taking all these aspects into account, in the present work, *Santolina insularis* essential oil was incorporated in liposomes and PEVs and their physico-chemical properties and skin delivery capability were tested. Liposomes were prepared using hydrogenated soy phosphatidylcholine (P90H), which has a high transition temperature (~50°C). The PEV formulations were obtained by adding propylene glycol (PG-PEVs) or ethylene glycol (EG-PEVs) to the water phase (10% v/v). The ability of the glycols to improve vesicle performances and stability has been previously probed using synthetic drugs (e.g., diclofenac and tretinoin), natural active molecules (e.g., quercetin and phycocyanin), and also a phytocomplex extracted from Fraxinus angustifolia [16–21].

To better understand the effect of the essential oil on the lamellar structure, all vesicles were deeply characterized combining the information obtained with different techniques: cryogenic transmission electron microscopy (cryo-TEM), dynamic and electrophoretic light scattering, turbiscan optical analyser (TurbiScan Lab®) and Small/Wide-Angle X-ray Scattering (SAXS and WAXS). The results allowed us to get a complete picture of *Santolina insularis* essential oil nanocarriers and to predict their feasibility as skin delivery systems. Moreover, the ability of PEVs to transport the essential oil through the skin was evaluated by confocal laser scanning microscopy (CLSM), using fluorescent vesicles. In addition, vesicle biocompatibility was tested in human keratinocytes.

2. Experimental

2.1. Materials

Hydrogenated soy phosphatidylcholine (Phospholipon® 90H, P90H) and 1,2-dioleolyl-sn-glycero-3-phosphoethanolamine-N-lissamine-sulfo-rhodamineB (Rho-PE) were purchased from Lipoid GmbH (Ludwigshafen, Germany). Phosphate buffer solution (PBS; Na_2HPO_3 / KH_3PO_3 in water, pH 7) was purchased from Carlo Erba Reagents (Milan, Italy). Cholesterol (CHOL), 5(6)-carboxyfluorescein (CF), Hoechst 33258, propylene glycol (PG), ethylene glycol (EG) and all other reagents were purchased from Sigma-Aldrich (Milan, Italy).

2.2. Plant material and essential oil preparation

Santolina insularis (Gennari ex Fiori) Arrigoni was collected during the flowering period (June 2013) in the South of Sardinia (Iglesiente subregion). A voucher specimen (CAG 732) has been deposited in the Herbarium of Botany and Botanical Garden Division of the University of Cagliari, Italy.

The aerial parts were air-dried at 40°C for two days, with forced ventilation. Prior to use, the matter was ground with a Malavasi mill (Bologna, Italy) and steam distilled (4 h) in a circulatory Clevenger-type apparatus according to the European Pharmacopoeia (Council of Europe, 1997).

2.3. GC-FID and GC-MS analyses

The identification of the components of the essential oil was carried out by gas chromatography (GC-FID) and gas chromatography-mass spectrometry (GC-MS).

GC-MS analysis was carried out using a gas chromatograph (Agilent, Model 6890N, Palo Alto, USA) using an Agilent HP5-MS fused silica column (5% phenyl-methylpolysiloxane, 30 m × 0.25 mm i.d., film thickness 0.25 μm). The GC conditions included programmed heating from 60 to 246°C at 3°C/min, followed by 20 min under isothermal conditions. The injector was maintained at 250°C. Helium was the carrier gas, at 1.0 ml/min. Samples were diluted in hexane (1:100) and injected (1 μl) in the split mode (1:20). The GC was fitted with a quadrupole mass spectrometer with an Agilent model 5973 detector. The MS conditions

were: ionization energy, 70 eV; electronic impact ion source temperature, 200°C; quadrupole temperature, 150°C; scan rate, 3.2 scan/s; mass range, 30-480 u. The software used to handle and analyse mass spectra and chromatograms was an Agilent MSD ChemStation E.01.00.237. The linear retention indices (RIs) for all the compounds were determined by injection of a hexane solution containing the C8-C26 series of n-alkanes and compared with those of authenticated samples from our database [22]. The identification of the essential oil constituents was accomplished by the comparison of their retention indices and their mass spectra from a home-made library or from literature data and mass spectra databases, including HPCH2205 [23] and W8N05ST (NIST/EPA/NIH 2005, Mass spectral library; National Institute of Standard and Technology, Gaithersburg).

Analytical GC was carried out in a gas chromatograph (Agilent, Model 7890A, Palo Alto, USA), equipped with a flame ionization detector (FID), an autosampler (Agilent, Model 7683B), Agilent HP5 fused silica column (5% phenyl-methylpolysiloxane, 30 m × 0.25 mm i.d., film thickness 0.25 μm), and a Agilent ChemStation software system. Oven temperature program: from 60 to 250ºC (3 ºC/min), 250ºC (20 min); injector temperature: 250ºC; carrier gas: helium at 1.0 ml/min; splitting ratio 1:10; detectors temperature: 300ºC. Percentages of individual components were calculated based on GC peak areas without FID response factor corrections.

2.4. Vesicle preparation

For the preparation of liposomes, PG- and EG-PEVs, P90H, cholesterol and *Santolina insularis* essential oil were dispersed in PBS or PG/PBS or EG/PBS (10% v/v; Table 2). Empty vesicles were also prepared as controls. The dispersions were sonicated (5 s on and 2 s off, 30 cycles; 12 microns of probe amplitude) with a high intensity ultrasonic disintegrator (Soniprep 150, MSE Crowley, London, UK). The vesicles were separated from the non-entrapped oil and non-aggregated phospholipid by dialysis. Samples (1 ml) were loaded into

dialysis tubing (Spectra/Por® membranes: 12-14 kDa MW cut-off, 3 nm pore size; Spectrum Laboratories Inc., DG Breda, The Netherlands) and dialysed against 3 l of PBS (for liposomes) or the appropriate glycol/PBS mixture (for PEVs), which was refreshed once during 2 h at 25°C.

Drug entrapment efficiency (EE%), expressed as the percentage of the drug found after dialysis versus the amount initially used, was analyzed at 310 nm using a UV-Visible spectrometer (Lambda 25, Perkin Elmer, MA, USA).

The phospholipid content of the vesicle dispersions was determined by the Stewart assay, a colorimetric technique that is based on the ability of phospholipids to form a complex with ammonium ferrothiocyanate [24]. First, a calibration curve was built: a series of chloroform solutions with known concentrations of P90H were treated with an aqueous solution containing ferric chloride and ammonium thiocyanate (0.1 N) and used to determine the P90H concentration in the vesicle formulations. To this purpose, both non-dialysed and dialysed samples were properly diluted in chloroform (1:20000), added to the ammonium ferrothiocyanate solution, and the absorbance into the organic phase was measured spectrophotometrically at 485 nm. The aggregation efficiency (AE%) represented the amount of aggregated phospholipid (after dialysis), expressed as the percentage of the amount initially used.

2.5. Vesicle characterization

Vesicle formation and morphology were checked by cryogenic transmission electron microscopy (cryo-TEM). An EM grid (Agar scientific, UK) with holey carbon film was held in tweezers and 4-5 μL of sample was applied on the grid. The tweezers were mounted in an automatic plunge freezing apparatus (Vitrobot, FEI, The Netherlands) to control humidity and temperature. After blotting, the grid was immersed in a small metal container with liquid ethane, which was cooled from outside by liquid nitrogen. The speed of cooling was such that

ice crystals did not have time to form. Observation was made at -170°C in a Tecnai F20 microscope (FEI, Eindhoven, The Netherlands) operating at 200 kV, equipped with a cryo-specimen holder Gatan 626 (Warrendale, PA, USA). Digital images were recorded with an Eagle (FEI) camera, 4098×4098 pixels. Magnification between 20000-30000×, using a defocus range of -2 to -3 µm.

The average diameter and polydispersity index (PI) of vesicles were determined by Dynamic Light Scattering (DLS) using a Zetasizer nano-ZS (Malvern Instruments, Worcestershire, UK). PI is a number calculated from the Cumulants analysis of the DLS-measured intensity autocorrelation function and describes the width of particle size distribution (or relative variance). The terms polydispersity (i.e., the standard deviation or width of the Gaussian distribution, or absolute polydispersity) and %polydispersity (i.e., the coefficient of variation = $PI^{1/2}$ × 100, or relative polydispersity) are derived from the PI and can all be used to describe the homogeneity of a particulate system.

The zeta potential was estimated using the Zetasizer nano-ZS, which converts the electrophoretic mobility by means of the Smoluchowski approximation of the Henry equation. Samples (n=6) were diluted (1:100) with PBS, or glycols/PBS (10% v/v) when appropriate, and analyzed at 25°C. Three runs in the automatic mode were performed, with the software determining automatically the most appropriate duration of each run (a minimum of 10 and a maximum of 100 subruns).

2.6. Stability study

The stability of the vesicles was evaluated by measuring vesicle average size and PI over 90 days at room temperature. In addition, the TurbiScan Lab® Expert optical analyser equipped with an ageing station (Formulaction, Paris, France), was used to determine the accelerated stability of the vesicular dispersions, by monitoring the samples under realistic conditions (without mechanical stress or dilution) [25,26]. The instrument scans the entire height of the

sample (λ = 880 nm), acquiring transmission and backscattering data every 40 μm, and shows the backscattering variation (ΔBS) in the three sections (bottom, middle and top) of the cell. Sample variations at the bottom and top are linked to migration phenomena (sedimentation and creaming); variations in the middle are mainly related to changes in particle size. The analyses were performed at 25°C every 3 h for 15 days.

2.7. Small/Wide-Angle X-ray Scattering (SAXS / WAXS)

SAXS and WAXS measurements were performed at the BL11-NCD (Non-Crystalline Diffraction) beamline at ALBA synchrotron facility (Cerdanyola del Vallès, Barcelona, Spain). The X-ray beams had flux of 10^{12} photons per second at an energy of 10 keV, and wavelength of 0.124 nm. *q* range was 0.09-4.77 nm^{-1}. The samples were loaded in a glass capillary mounted on a motorized sample-stage, thermostated at 25°C, which allowed the sample to be aligned and oriented in the beam. Two dimensional X-ray scattering patterns were acquired using an ADSC Quantum 210r CCD detector. Exposure time per frame was 5 sec. The images were radially averaged and summed. Two series of diffraction patterns were obtained from the same capillary with a separation of 500 μm to check for reproducibility and possible radiation damage.

SAXS patterns were analysed using a home-made fitting procedure based on a Gaussian description of the bilayers [27,28] and using a Levenberg-Marquardt minimization scheme [29]. Further, we introduced the possibility of dissymmetry in the bilayer by numeric Fourier transformation of asymmetric bilayers, as suggested by Kučerka et al [30].

The bilayer was constructed using a negative Gaussian concentric with the bilayer corresponding to the methyl groups of the hydrocarbon chains (eq. 1):

$$G_m(z) = \frac{1}{\sqrt{2\pi}} \rho_m \exp\left(-\frac{z^2}{\sigma_m^2}\right) \qquad \text{eq. 1}$$

and another negative electron density contribution corresponding to the hydrocarbon chains introduced through an error function (eq. 2-3):

$$HC(z) = \rho_{CH_2}\left[(erf\,(z, z_{CH_21}, \sigma_{CH_21}) - (erf\,(z, z_{CH_22}, \sigma_{CH_22})\right] \quad \text{eq. 2}$$

$$erf\,(z, z_{CH_2i}, \sigma_{CH_2i}) = \frac{2}{\sqrt{\pi}}\int_0^{\frac{Z - Z_{CH2i}}{\sqrt{2\sigma_{CH2i}}}} \exp\left[-x^2\right]dx \quad \text{eq. 3}$$

The mean electron density of the hydrocarbon region was used as a constraint for the depth (ρ_m) and width of the Gaussian (σ_m) and error functions (ρ_{CH2}, σ_{CH2}, Z_{hi}). The polar heads were represented by two Gaussian functions with electron density above 0 (eq. 4-5):

$$G_{h1}(z) = \frac{1}{\sqrt{2\pi}}\rho_{h1}\exp\left(-\frac{\left(z - z_{h1}\right)^2}{\sigma_{h1}^2}\right) \quad \text{eq. 4}$$

$$G_{h2}(z) = \frac{1}{\sqrt{2\pi}}\rho_{h2}\exp\left(-\frac{\left(z - z_{h2}\right)^2}{\sigma_{h2}^2}\right) \quad \text{eq. 5}$$

In such fits, the amplitude of the methyl groups tended to zero (σ_m), and was restricted not to go below 3 Å. The position of the error function Z_{CH2i} was also constrained to be below the center of the Gaussian representing the polar head by the amplitude of that Gaussian (i.e., $Z_{CH2i} = Z_{hi} - \sigma_{hi}$, and the amplitude of the error function σ_{CH2i} was also restricted to the value of 3 Å. The fitting procedure using the Levenberg-Marquardt minimization scheme was started using a symmetric model; in a second step, dissymmetry was allowed and the fit was retained if a significant decrease in chi-square χ^2 was obtained. See ref. [29] for further details on the fitting procedures.

The derived parameters were obtained as follows: the length of the bilayer hydrocarbon chain (d_c) was obtained from the position of the error function describing the hydrophobic chains (Figure S1); Z_H corresponded to the center of the polar heads' Gaussian (Figure S1), and σ_H to

the amplitude of those Gaussians; the area per molecule (*A*) was obtained from the number of electrons divided by the integral of the electronic density corresponding to the hydrophobic contribution; *A* was used to further check for the value of hydrophobic thickness by dividing the hydrophobic volume by the area per molecule. The total bilayer thickness (d_B) was calculated as the distance between the extreme positions at which the polar head Gaussians reached their half maximum values (Figure S1); the number of water molecules (N_w) was obtained from the total volume of the bilayer minus the volume of the phospholipid and cholesterol.

2.8. Confocal Laser Scanning Microscopy (CLSM)

The vesicular formulations were labelled with a lipophilic fluorescent marker (Rho-PE; 0.035 mg/ml), loaded with a hydrophilic fluorescent marker (CF; 0.025 mg/ml) and applied on pig skin using Franz diffusion cells, as previously reported [31]. At regular time intervals (2, 4, 8, 24 h), skin specimens were gently washed with distilled water, the diffusion area punched out and frozen at -80 °C. Sections of the skin (7 μm thickness) were cut with a cryostat (Leica CM1950, Barcelona, Spain) orthogonally (in the z axis) to the surface, and examined under a FluoView FV1000 inverted confocal microscope (Olympus, Barcelona, Spain) equipped with an Ultraviolet/Visible light laser. Using an UplanSApo 20x objective NA 0.75, images with a field size of 1024×1024 μm were generated. CF and Rho-PE were excited at 600 nm and 559 nm, and detected at 640 nm and 578 nm, respectively.

2.9. Cell viability studies (MTT assay)

Human keratinocytes were grown as monolayers at 37°C, 100% humidity and 5% CO_2, using RPMI1640 medium (Life Technology, Monza, Italy) with high glucose, supplemented with 10% (v/v) fetal bovine serum, penicillin (100 U/ml), and streptomycin (100 μg/ml) (Life Technologies, Monza, Italy) as a growth medium. Cells were seeded into 96-well plates at a density of $7.5x10^3$ cells/well. After 24 h of incubation, cells were treated for 8, 24 and 48 h

with different concentrations (50, 20, 10, 2, 1 μg/ml) of the *Santolina insularis* essential oil, as obtained by properly diluting the formulations or the oil/PBS blend with the cell culture medium. Cell viability was determined by adding MTT [3(4,5-dimethylthiazolyl-2)-2, 5-diphenyltetrazolium bromide] (200 μl, 0.5 mg/ml) to each well, dissolving (after 2 h) the formed formazan crystals with DMSO and measuring the absorbance at 570 nm with a microplate reader (Synergy 4, ReaderBioTek Instruments, AHSI S.p.A, Bernareggio, Italy). All experiments were repeated at least three times and in triplicate. Results are shown as percent of cell viability in comparison with non-treated control cells (100% viability).

2.10. Statistical analysis of data

Results are expressed as the mean±standard deviation (SD). Multiple comparison of means (Tukey's test) were used to substantiate statistical differences between groups, while Student's t-test was used to compare two samples. Significance was tested at the 0.05 level of probability (p). Data analysis was carried out with the software package R, version 2.10.1.

3. Results and discussion

3.1. Essential oil analysis

The steam distillation of the aerial parts of *Santolina insularis* gave a light yellow essential oil. The yield of the oil, expressed as the percentage by weight of the oil versus the weight of the material charged in the extractor, was ~3%. The essential oil was analyzed by GC-MS for qualitative and quantitative analysis (Table 1). 38 different compounds were identified, representing 93% of the total oil. In Table 1, only the compounds ≥1% are reported. The essential oil was predominantly composed of hydrocarbon monoterpenes (51.9%), oxygenated monoterpenes (14.6%), hydrocarbon sesquiterpenes (16.1%), oxygenated sesquiterpenes (10.0%). The most abundant terpenes were β-phellandrene (22.6%), myrcene (11.4%) and curcumenes (12.1%), in agreement with the findings of Gnavi et al [32].

3.2. Vesicle characterization

In a previous work, *Santolina insularis* essential oil was incorporated in P90H liposomes, which were proved effective in protecting the the essential oil from degradation, and in inactivating the herpes simplex virus [12]. In the present work, *Santolina insularis* essential oil was incorporated in liposomes and PEVs, representing a promising system for enhanced skin delivery. The composition of the vesicles is reported in Table 2. Previous studies demonstrated the capability of propylene and ethylene glycol containing vesicles to increase the stability, skin delivery and anti-inflammatory efficacy of different drugs and natural products [16,18,19,21]. In this paper, liquid and lipophilic mono and sesquiterpenes from *Santolina insularis* essential oil were incorporated in glycol-PEVs, and their location and effect on the vesicle bilayer were investigated.

Cryo-TEM micrographs showed that both empty and *Santolina insularis* essential oil-loaded liposomes and PEVs were predominantly unilamellar, polyhedral (faceted) vesicles (Figure 1A, B), whose occurrence was particularly evident in PEVs. The existence of these peculiar nanostructures is broadly reported in the literature, although the origin of the faceted morphology has not been fully clarified yet.

The physico-chemical features of empty liposomes and PEVs were very similar (Table 3): the mean diameter, estimated by DLS, was around 100 nm with small SD values, indicating that the average size of the different replicates (n=6) was highly reproducible and repeatable; PI was ~0.32 and zeta potential was ~-12 mV. The incorporation of the essential oil within the vesicles led to a slight increase in size (~115 nm), and a decrease in polydispersity (PI~0.15), while the effect of the glycols was negligible ($p>0.05$). Nevertheless, it should be noted that, especially for polydisperse systems, DLS can provide only an estimate of the average size. This is an intensity-based calculated value, which is weighed according to the scattering intensity of each particle fraction. As such, the intensity distribution can be somewhat misleading, in that the presence of larger particles can dominate the distribution, hiding the

smallest particles. Therefore, a calculation of the vesicle diameter was carried out by cryo-TEM observations. As expected, the values were smaller and with high SD, revealing the actual polydispersity of the samples (Table 3).

The results of the entrapment efficiency of *Santolina insularis* essential oil indicate that it can be incorporated in good amounts in the prepared vesicular dispersions, especially in liposomes (EE% ~70; Table 3). In agreement with previous results, PEVs possessed lower EE% (~50; Table 3), due to a high solubilization of the essential oil in the glycol/PBS intervesicle medium, which reduced the amount of the essential oil entrapped within the PEVs. The aggregation efficiency of P90H was almost similar in all the formulations (AE ~71%; Table 3), either empty or essential oil-loaded liposomes and PEVs.

The TurbiScan Lab® was employed to evaluate the accelerated stability behaviour of the essential oil-loaded liposomes and PEVs. An evaluation of the destabilization processes occurring in the colloidal dispersions was made by measuring the backscattering (BS) in the samples [25,26]. Figure 1C depicts the BS profiles for the vesicle dispersions: BS and time are shown on the ordinate, while the height of the cell is indicated on the abscissa of the graph. The first curve is displayed in pink, the last one in red. When the BS values are within the ±2% interval, the stability of the formulations can be considered optimal. The BS of liposomes increased slightly in the whole sample (~1.7%), indicating a good stability of the formulation and the absence of migration phenomena, such as creaming or sedimentation (Figure 1C). The variation of BS can be ascribed to an increase in vesicle size. PG-PEVs showed a similar behavior (BS ~2%; Figure 1C). EG-PEVs were the most stable formulation: no sign of particle migration was observed, and the increase in vesicle size was minimum (Figure 1C). The variation of BS was ~-0.4%. Such negative value is very common in samples with BS close to zero, and is due to an error associated with the instrument since,

according to Rayleigh diffusion, BS flux increases with the increase in size when the particle size is smaller than the wavelength of the light used to measure the samples (880 nm).

SAXS scattering curves of empty liposomes and PEVs showed the typical shape of unilamellar vesicles (Figure 2A, B). However, in the case of PG-PEVs, the use of a small percentage (4%) bilamellar vesicles improved the fittings, thus indicating that the presence of a minor population of oligolamellar structures better describes the sample. The fits were very good up to 2 nm^{-1}, but above this threshold they were unable to capture the fine features of the low intensity region. This is reflected in the values of reduced χ^2 (for purely statistical noise $\chi^2=1$; for nearly perfect fitting $\chi^2<2$), which were in the range from 5 to 10 (poor fitting). This implies that our model did not capture fine features below 1 nm.

While empty liposomes and PG-PEVs showed a minimum close to 0 (around 0.4 nm^{-1}), this minimum was not so deep for empty EG-PEVs (Figure 2A). Moreover, we found a relatively small asymmetry in the electron density profiles corresponding to the best fits of EG-PEVs (Figure 2C). The reduction of this dip in the SAXS curves and the increased asymmetry of unilamellar vesicles may be caused by different factors: the bending of the membrane in small vesicles, however, this effect is significant only when the size is below 50 nm in diameter [33]; the bilayer asymmetry [30] or the heterogeneity in bilayer thickness. So far, the latter has not been found in the literature.

The minimum around 0.4 nm^{-1} was clearly shallower for the *Santolina insularis* essential oil-loaded vesicles, as shown in Figure 2B, reflecting the asymmetry of the bilayers. The asymmetry was not very strong and may be due to a different partition of the constituents in the interior and exterior of the vesicles. There was no sign of multilamellarity in the SAXS curves, indicating that the vesicles were truly unilamellar, or if more than one lamella existed, there was no correlation between adjacent lamellae. As can be observed in Figure 2B, the fits produced asymmetric bilayers, and this asymmetry was larger for EG-PEVs than for PG-

PEVs and liposomes, as also reflected in the width of the Gaussians corresponding to the headgroups of the two leaflets of the bilayers (Figure 2D). The overall effect was an increase in the polar head length. The faceting of vesicles observed in cryo-TEM images of *Santolina insularis* essential oil-loaded vesicles might be correlated to the smearing of the first minimum in the SAXS spectra and the asymmetric fit, which can be due to three different effects: a) the limited domain of flat bilayer pieces, b) the bending of the bilayer between flat domains (having an effect when the radius of curvature of the bending is below 25 nm as in the curvature of small unilamellar vesicles), and c) because of the asymmetry of the bilayer in the bending parts between domains. Since a model for the faceting of vesicles is not available yet, we only used the asymmetric bilayers model. Therefore, our results have to be regarded as a first approximation. In previous findings, the faceting of otherwise smooth, rounded vesicles, seemed to occur when the lipids constituting the bilayer were below the gel (L_β) to fluid (L_α) transition temperature [34–37] and to be produced by the induction of asymmetry in rigid bilayer domains with ordering in the plane of the bilayer [38]. From the analysis of the WAXS domains of our formulations, the presence of a weak peak at around 1.52 $Å^{-1}$ was noticed, which coincides with the peak attributed to L_β or $L_{\beta'}$ (Figure 2E, F) [39]. Because of the low concentration of the phospholipid in the samples, this signal could be distinctively seen only after the background subtraction. Hence, these findings are in agreement with the previous assumptions, allowing us to conclude that the faceting can be due to the coexistence of fluid and gel phases.

The main parameters obtained from the fits are listed in Table 4. The use of PG or EG produced an increase in the amplitude of the polar heads (σ_H), while the addition of *Santolina insularis* essential oil had a significant effect on σ_H only in the absence of PG or EG. Both the use of the cosolvent and the incorporation of the essential oil increased the area per molecule (*A*), with respect to empty liposomes. Conversely, a slight decrease in the length of the bilayer

hydrocarbon chain (d_c) was observed in the presence of PG and EG, which was mitigated after incorporating the essential oil (except for EG-PEVs). The mean distance of the polar head to the centre of the bilayer (Z_H) displayed a similar behaviour, though the decrease was even less marked. Both the cosolvents and the essential oil had also a slight tendency to increase the mean polar head amplitude, with a significant effect of the essential oil in increasing the dissymmetry of the polar heads. We can conclude that *Santolina insularis* essential oil was embedded within the vesicle bilayers with relatively mild effects, the most notable being the introduction of dissymmetry in the bilayers, which can still be considered quite symmetric, without affecting the faceted structure of P90H vesicles.

Altogether, the data from morphology, size distribution, zeta potential, entrapment and aggregation efficiency, bilayer structure and vesicle stability studies, disclosed that, due to its composite lipophilic nature, *Santolina insularis* essential oil can be considered as a constituent of the vesicle structure, forming a new active assembly.

3.3. CLSM study of vesicle skin delivery

The vesicles were labelled with Rho-PE, a fluorescent phospholipid, and a hydrophilic, fluorescent probe, CF. Fluorescent vesicles were applied on new born pig skin using Franz diffusion cells. At the end of the experiments (at 2, 4, 8 and 24 h), the penetration extent and distribution of the markers into the skin strata were evaluated using the confocal microscope [31]. Rho-PE appeared in red and CF in green; the presence of both markers gave a yellow fluorescence, which is indicative of the simultaneous presence of lipophilic and hydrophilic vesicular components and can be predictive of the potential penetration of intact vesicles through the skin barrier. Figure 3 illustrates the images of fluorescent liposomes (control), EG- and PG-PEVs applied onto the skin at the different exposure times. As can be seen, the accumulation of the probes into the different cutaneous strata is time-dependent for all the vesicles. Using liposomes, the green fluorescence, mimicking the hydrophilic content of the

vesicles, was the predominant signal, mostly detected in the epidermis, indicating the penetration of CF alone. After 8 h, both Rho-PE and CF were visible in the epidermis as yellow fluorescence, being more evident at 24 h. These findings support the hypothesis that liposomes are adsorbed on the skin surface, where they can fuse or mix with the skin lipids, thus releasing their content.

On the contrary, using PEVs, after 4 h the skin exhibited a predominance of red fluorescence, with some yellow areas, while after 8-24 h, a widespread yellow fluorescence were observed in the epidermis and a diffused red fluorescence in the dermis, suggesting a different mechanism of penetration than for liposomes. As previously reported, PEVs are supposed to fuse with the lipids of the superficial skin, acting as penetration enhancers and facilitating the diffusion of intact vesicles in the viable epidermis, where they form a depot from which the loaded drug is slowly released.

3.4. In vitro cell viability

Cell viability studies on keratinocytes were performed to ascertain the biocompatibility of the *Santolina insularis* essential oil vesicles. The essential oil is composed of different terpenes, which were reported to be toxic. The level of metabolically active mitochondrial dehydrogenase enzymes was evaluated in vitro according to the MTT assay. The cell survival was assayed after incubation with the essential oil loaded in vesicles at 8, 24 and 48 h. The results confirmed the good biocompatibility of all formulations, liposomes and PEVs, as the viability was ≥100% up to 48 h (Figure 4). By contrast, cell viability in the presence of the free oil was approximately 100% after 8 h, but decreased to 80% after 24 and 48 h, regardless of the concentration used. Hence, these findings point to the fact that the prepared vesicles were able to reduce the intrinsic toxicity of the essential oil.

4. Conclusion

In this work, *Santolina insularis* essential oil was incorporated in polyhedral, faceted liposomes and PEVs aiming at improving its biological activity. Thanks to their peculiar properties, *Santolina insularis* essential oil-loaded vesicles, especially EG-PEVs, can be proposed as a safe delivery system for drugs, or as a topical antibacterial formulation itself.

Acknowledgments

SAXS/WAXS experiments were performed at the BL11-NCD beamline at ALBA Synchrotron with the collaboration of ALBA staff. The beamtime at ALBA was kindly provided within the approved proposal n. 2013110789.

This work was supported by a grant from Programma di Sviluppo Rurale 2007-2013 PSR Sardegna-MISURA 124, NANOFITOCARE, determinazione n. 4230/14.

Dr. Pons acknowledges financial support from MINECO-CTQ2013-41514-P.

References

[1] J.L. Ríos, M.C. Recio, Medicinal plants and antimicrobial activity., J. Ethnopharmacol. 100 (2005) 80–4.

[2] L. Kokoska, Z. Polesny, V. Rada, A. Nepovim, T. Vanek, Screening of some Siberian medicinal plants for antimicrobial activity, J. Ethnopharmacol. 82 (2002) 51–53.

[3] C.F. Carson, T.V. Riley, Antimicrobial activity of the major components of the essential oil of Melaleuca alternifolia, J. Appl. Bacteriol. 78 (1995) 264–269.

[4] S. Cosentino, C.I.G. Tuberoso, B. Pisano, M. Satta, V. Mascia, E. Arzedi, et al., In-vitro antimicrobial activity and chemical composition of Sardinian Thymus essential oils, Lett. Appl. Microbiol. 29 (1999) 130–135. [5] C. Sinico, A. De Logu, F. Lai, D. Valenti, M. Manconi, G. Loy, et al., Liposomal incorporation of Artemisia arborescens L. essential oil and in vitro antiviral activity, Eur. J. Pharm. Biopharm. 59 (2005) 161–168.

[6] B. Marongiu, A. Piras, S. Porcedda, D. Falconieri, A. Maxia, M.J. Gonçalves, et al., Chemical composition and biological assays of essential oils of Calamintha nepeta (L.) Savi subsp. nepeta (Lamiaceae)., Nat. Prod. Res. 24 (2010) 1734–42.

[7] A. Maxia, C. Sanna, A. Piras, S. Porcedda, D. Falconieri, M.J. Gonçalves, et al., Chemical composition and biological activity of Tanacetum audibertii (Req.) DC. (Asteraceae), an endemic species of Sardinia Island, Italy, Ind. Crops Prod. (2014).

[8] A. Piras, D. Falconieri, E. Bagdonaite, A. Maxia, M.J. Gonçalves, C. Cavaleiro, et al., Chemical composition and antifungal activity of supercritical extract and essential oil of Tanacetum vulgare growing wild in Lithuania., Nat. Prod. Res. 28 (2014) 1906–9.

[9] A. Salminen, M. Lehtonen, T. Suuronen, K. Kaarniranta, J. Huuskonen, Terpenoids: natural inhibitors of NF-kappaB signaling with anti-inflammatory and anticancer potential., Cell. Mol. Life Sci. 65 (2008) 2979–99.

[10] A. De Logu, G. Loy, M.L. Pellerano, L. Bonsignore, M.L. Schivo, Inactivation of HSV-1 and HSV-2 and prevention of cell-to-cell virus spread by Santolina insularis essential oil, Antiviral Res. 48 (2000) 177–185.

[11] G. Cherchi, D. Deidda, B. De Gioannis, B. Marongiu, R. Pompei, S. Porcedda, Extraction ofSantolina insularis essential oil by supercritical carbon dioxide: influence of some process parameters and biological activity, Flavour Fragr. J. 16 (2001) 35–43.

[12] D. Valenti, A. De Logu, G. Loy, C. Sinico, L. Bonsignore, F. Cottiglia, et al., Liposome-incorporated santolina insularis essential oil: preparation, characterization and in vitro antiviral activity., J. Liposome Res. 11 (2001) 73–90.

[13] M. Sherry, C. Charcosset, H. Fessi, H. Greige-Gerges, Essential oils encapsulated in liposomes: a review, J. Liposome Res. 23 (2013) 268–275.

[14] F. Cuomo, M. Mosca, S. Murgia, A. Ceglie, F. Lopez, Oligonucleotides and polynucleotides condensation onto liposome surface: effects of the base and of the nucleotide length., Colloids Surf. B. Biointerfaces. 104 (2013) 239–44.

[15] F. Cuomo, M. Mosca, S. Murgia, P. Avino, A. Ceglie, F. Lopez, Evidence for the role of hydrophobic forces on the interactions of nucleotide-monophosphates with cationic liposomes., J. Colloid Interface Sci. 410 (2013) 146–51.

[16] M. Manconi, S. Mura, C. Sinico, A.M. Fadda, A.O. Vila, F. Molina, Development and characterization of liposomes containing glycols as carriers for diclofenac, Colloids Surfaces A Physicochem. Eng. Asp. 342 (2009) 53–58.

[17] M. Manconi, C. Sinico, C. Caddeo, A.O. Vila, D. Valenti, A.M. Fadda, Penetration enhancer containing vesicles as carriers for dermal delivery of tretinoin, Int. J. Pharm. 412 (2011) 37–46.

[18] M. Chessa, C. Caddeo, D. Valenti, M. Manconi, C. Sinico, A.M. Fadda, Effect of Penetration Enhancer Containing Vesicles on the Percutaneous Delivery of Quercetin through New Born Pig Skin., Pharmaceutics. 3 (2011) 497–509.

[19] C. Caddeo, M. Chessa, A. Vassallo, R. Pons, O. Diez-Sales, A.M. Fadda, et al., Extraction, Purification and Nanoformulation of Natural Phycocyanin (from Klamath algae) for Dermal and Deeper Soft Tissue Delivery, J. Biomed. Nanotechnol. 9 (2013) 1929–1938.

[20] I. Castangia, M.L. Manca, P. Matricardi, C. Sinico, S. Lampis, X. Fernàndez-Busquets, et al., Effect of diclofenac and glycol intercalation on structural assembly of phospholipid lamellar vesicles, Int. J. Pharm. 456 (2013) 1–9.

[21] K. Moulaoui, C. Caddeo, M.L. Manca, I. Castangia, D. Valenti, E. Escribano, et al., Identification and nanoentrapment of polyphenolic phytocomplex from Fraxinus angustifolia: In vitro and in vivo wound healing potential., Eur. J. Med. Chem. 89 (2015) 179–88.

[22] H. van Den Dool, P. Dec. Kratz, A generalization of the retention index system including linear temperature programmed gas—liquid partition chromatography, J. Chromatogr. A. 11 (1963) 463–471.

[23] R.P. Adams, Identification of essential oil components by gas chromatography/quadrupole mass spectrometry, Allured Publishing Corporation, 2001.

[24] J.C.M. Stewart, Colorimetric determination of phospholipids with ammonium ferrothiocyanate, Anal. Biochem. 104 (1980) 10–14.

[25] M.L. Manca, I. Castangia, C. Caddeo, D. Pando, E. Escribano, D. Valenti, et al., Improvement of quercetin protective effect against oxidative stress skin damages by incorporation in nanovesicles., Colloids Surf. B. Biointerfaces. 123 (2014) 566–74.

[26] C. Lemarchand, P. Couvreur, C. Vauthier, D. Costantini, G. Ruxandra, Study of emulsion stabilization by graft copolymers using the optical analyzer Turbiscan, Int. J. Pharm. 254 (2003) 77–82.

[27] G. Pabst, M. Rappolt, H. Amenitsch, P. Laggner, Structural information from multilamellar liposomes at full hydration: Full q-range fitting with high quality x-ray data, Phys. Rev. E. 62 (2000) 4000–4009.

[28] P. Heftberger, B. Kollmitzer, F.A. Heberle, J. Pan, M. Rappolt, H. Amenitsch, et al., Global small-angle X-ray scattering data analysis for multilamellar vesicles: the evolution of the scattering density profile model., J. Appl. Crystallogr. 47 (2014) 173–180.

[29] J.S. Pedersen, Analysis of small-angle scattering data from colloids and polymer solutions: modeling and least-squares fitting, Adv. Colloid Interface Sci. 70 (1997) 171–210.

[30] N. Kučerka, M.-P. Nieh, J. Katsaras, Asymmetric Distribution of Cholesterol in Unilamellar Vesicles of Monounsaturated Phospholipids, Langmuir. 25 (2009) 13522–13527.

[31] M. Manconi, C. Caddeo, C. Sinico, D. Valenti, M.C. Mostallino, S. Lampis, et al., Penetration enhancer-containing vesicles: Composition dependence of structural features and skin penetration ability, Eur. J. Pharm. Biopharm. 82 (2012) 352–359.

[32] G. Gnavi, C.M. Bertea, M. Usai, M.E. Maffei, Comparative characterization of Santolina insularis chemotypes by essential oil composition, 5S-rRNA-NTS sequencing and EcoRV RFLP-PCR., Phytochemistry. 71 (2010) 930–6.

[33] J.A. Bouwstra, G.S. Gooris, W. Bras, H. Talsma, Small angle X-ray scattering: possibilities and limitations in characterization of vesicles, Chem. Phys. Lipids. 64 (1993) 83–98.

[34] M. Andersson, L. Hammarstroem, K. Edwards, Effect of Bilayer Phase Transitions on Vesicle Structure, and its Influence on the Kinetics of Viologen Reduction, J. Phys. Chem. 99 (1995) 14531–14538.

[35] P. Oliger, M. Schmutz, M. Hebrant, C. Grison, P. Coutrot, C. Tondre, Vesicle-Forming Properties of New Phospholipid Analogues Derived from N -Phosphonoacetyl- l -aspartate (PALA): Particle Features and Morphology in Relation with Alkyl Chain Lengths †, Langmuir. 17 (2001) 3893–3897.

[36] A. Dicko, P. Tardi, X. Xie, L. Mayer, Role of copper gluconate/triethanolamine in irinotecan encapsulation inside the liposomes., Int. J. Pharm. 337 (2007) 219–28.

[37] P. Nordly, K.S. Korsholm, E.A. Pedersen, T.S. Khilji, H. Franzyk, L. Jorgensen, et al., Incorporation of a synthetic mycobacterial monomycoloyl glycerol analogue stabilizes dimethyldioctadecylammonium liposomes and potentiates their adjuvant effect in vivo., Eur. J. Pharm. Biopharm. 77 (2011) 89–98.

[38] C.-Y. Leung, L.C. Palmer, B.F. Qiao, S. Kewalramani, R. Sknepnek, C.J. Newcomb, et al., Molecular crystallization controlled by pH regulates mesoscopic membrane morphology., ACS Nano. 6 (2012) 10901–9.

[39] A. Tardieu, V. Luzzati, F.C. Reman, Structure and polymorphism of the hydrocarbon chains of lipids: A study of lecithin-water phases, J. Mol. Biol. 75 (1973) 711–733.

FIGURE CAPTIONS

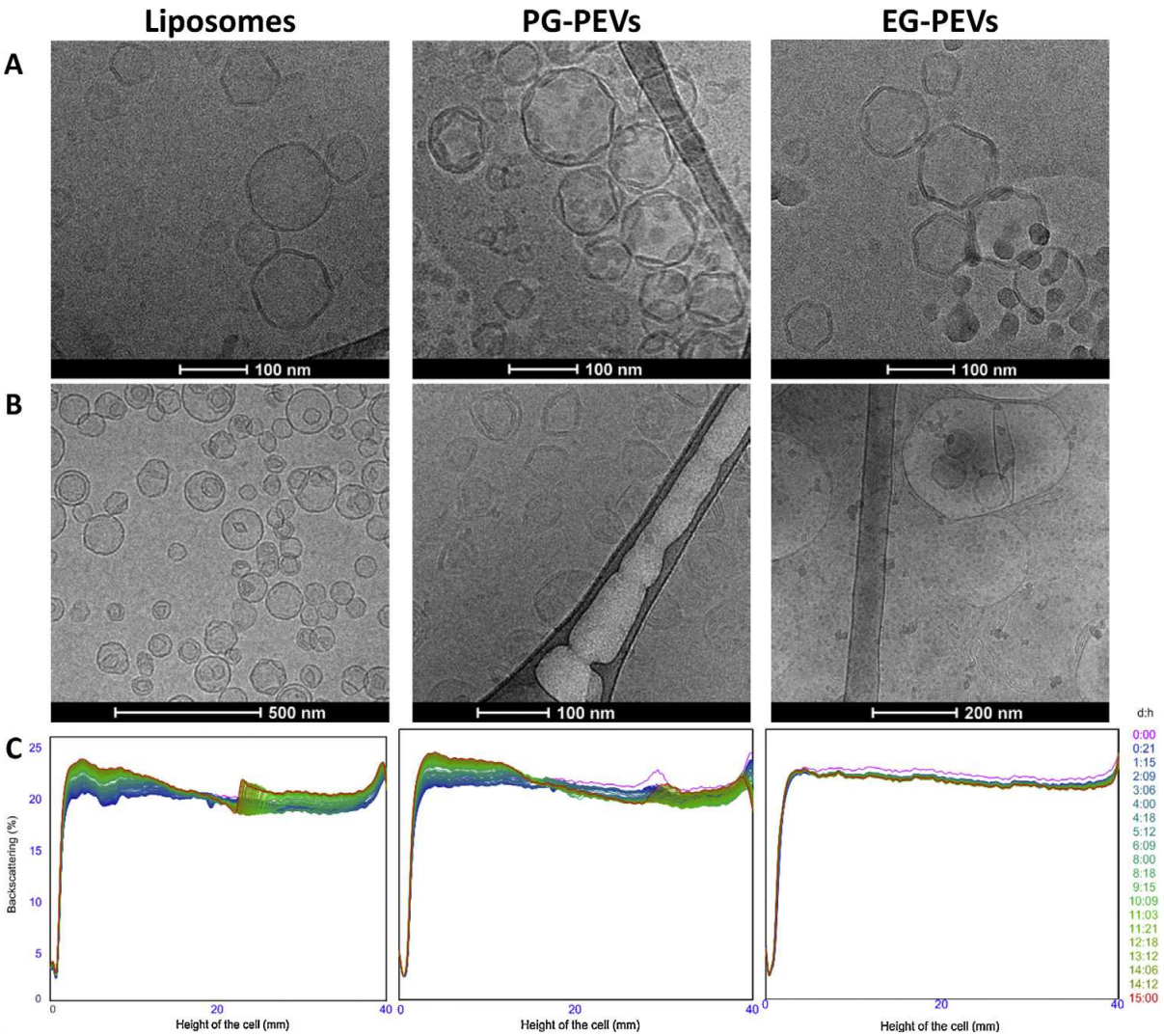

Fig. 1. Cryo-TEM micrographs of empty (A) and *Santolina insularis* essential oil-loaded liposomes and PEVs (B). Backscattering profiles of *Santolina insularis* essential oil-loaded liposomes and PEVs (C).

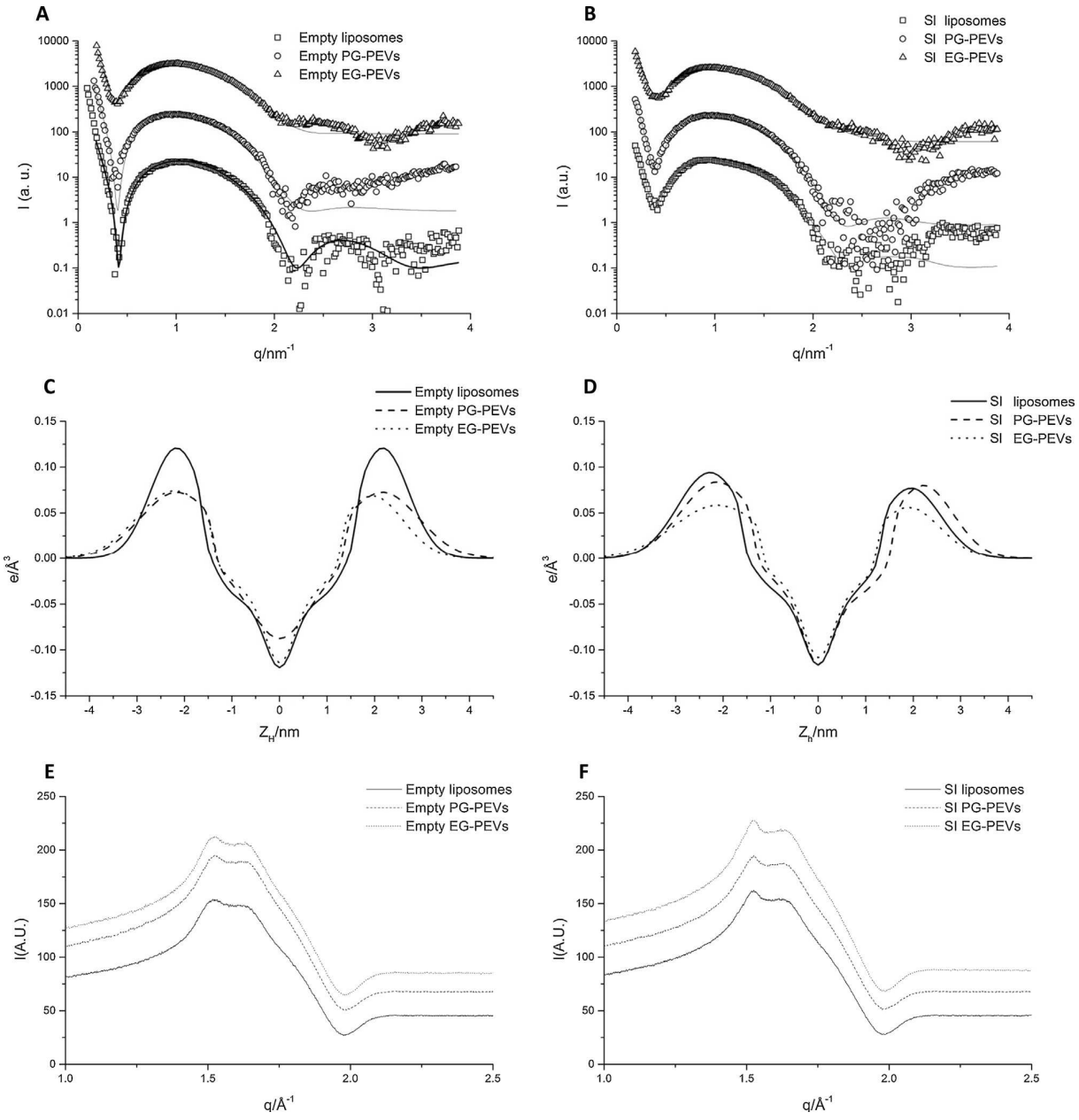

Fig. 2. SAXS profiles of empty (A) and *Santolina insularis* essential oil (SI)-loaded liposomes and PEVs (B). The data have been scaled multiplying by factors of 10 for clarity. The lines corresponds to the best fit of Gaussian bilayer models, see the text for details on the fitting. Electron density profiles corresponding to the best fits of empty (C) and *Santolina insularis* essential oil (SI)-loaded liposomes and PEVs (D) are presented.
WAXS profiles of empty (E) and *Santolina insularis* essential oil (SI)-loaded liposomes and PEVs (F).

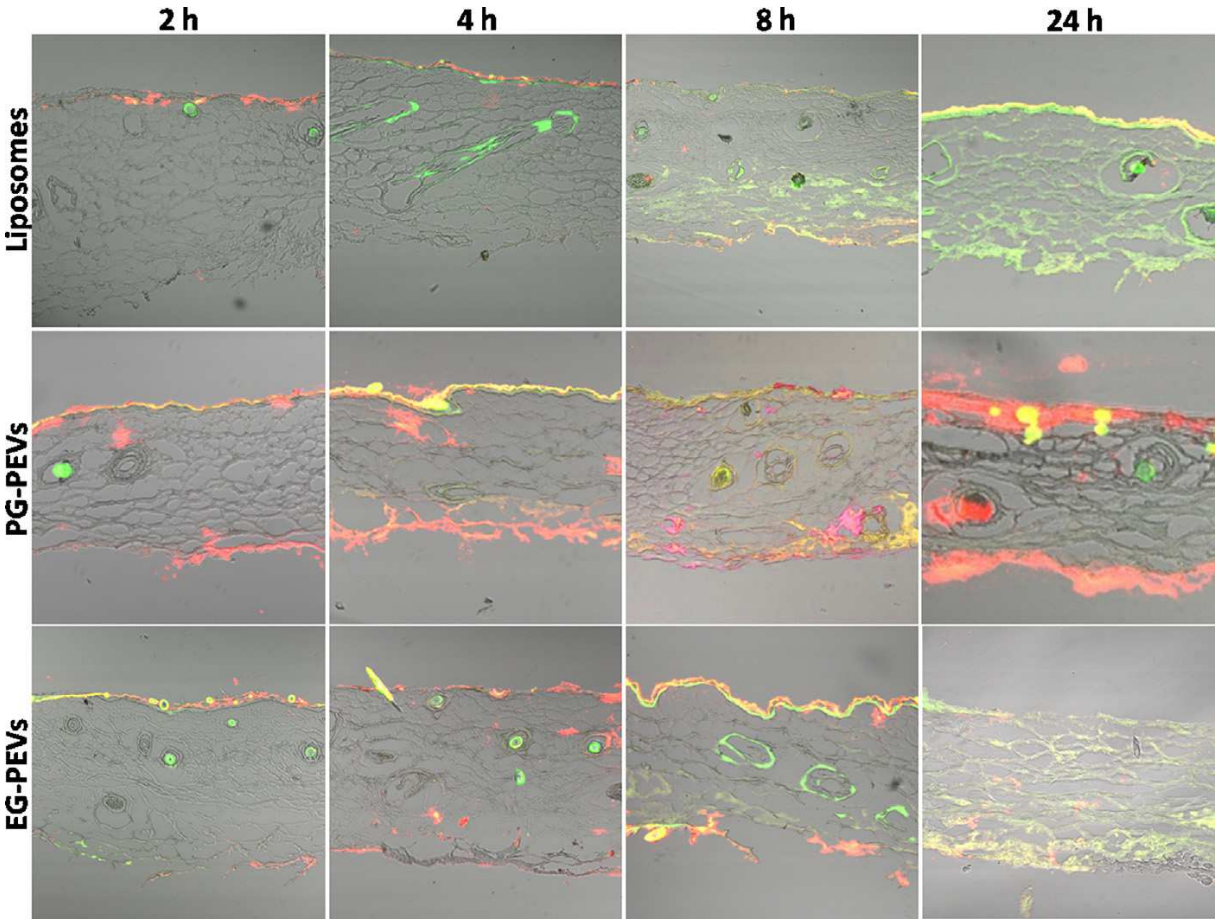

Fig. 3. CLSM images of pig skin after 2, 4, 8 and 24 h treatment with fluorescent liposomes (upper panel), PG-PEVs (middle panel) and EG-PEVs (lower panel) loaded with *Santolina insularis* essential oil. Images show the distribution of red (rhodamine) and green (carboxyfluorescein) fluorescence.

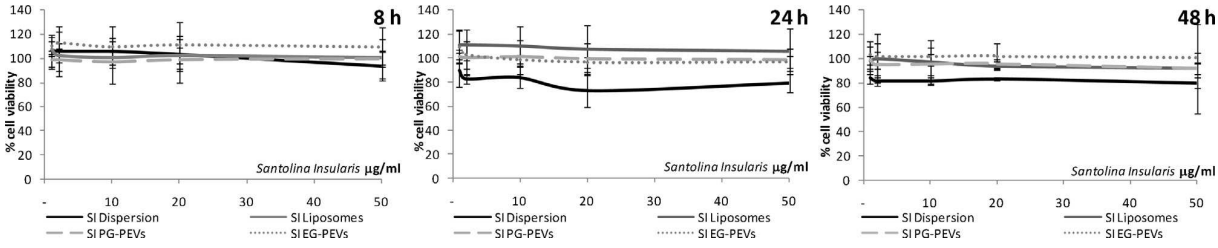

Fig. 4. Viability of human keratinocytes incubated for 8, 24 and 48 h with different concentrations (1, 2, 10, 20, 50 µg/ml) of *Santolina insularis* essential oil (SI) in liposomes and PEVs or dispersed in PBS.

SUPPLEMENTARY INFORMATION

Faceted phospholipid vesicles tailored for the delivery of *Santolina insularis* essential oil to the skin

Ines Castangia,[a] Maria Letizia Manca,[a] Carla Caddeo,[a,*] Andrea Maxia,[b] Sergio Murgia,[c] Ramon Pons,[d] Davide Demurtas,[e] Daniel Pando,[f] Danilo Falconieri,[b] José E. Peris,[g] Anna Maria Fadda,[a] Maria Manconi[a]

[a] Dept. Scienze della Vita e dell'Ambiente, Drug Science Division, University of Cagliari, 09124 Cagliari, Italy
[b] Dept. Scienze della Vita e dell'Ambiente, Botany and Botanical Garden Division, University of Cagliari, 09124 Cagliari, Italy
[c] Dept. Scienze Chimiche e Geologiche, CNBS and CSGI, University of Cagliari, Monserrato (CA), Italy
[d] Dept. Tecnologia Química i de Tensioactius, Institut de Química Avançada de Catalunya (IQAC-CSIC) 08034 Barcelona, Spain
[e] Interdisciplinary Center for Electron Microscopy, Ecole Polytechnique Fédérale de Lausanne, Station 12, 1015-Lausanne, Switzerland
[f] Dept. Ingeniería Química y Tecnología del Medio Ambiente, University of Oviedo, Oviedo, Spain
[g] Dept. Farmacia y Tecnologia Farmaceutica, University of Valencia, 46100-Burjassot, Valencia, Spain

*Corresponding author: Carla Caddeo

Dept. Scienze della Vita e dell'Ambiente, Drug Science Division, University of Cagliari, 09124 Cagliari, Italy

Tel.: +39 0706758582; fax: +39 0706758553; e-mail address: caddeoc@unica.it

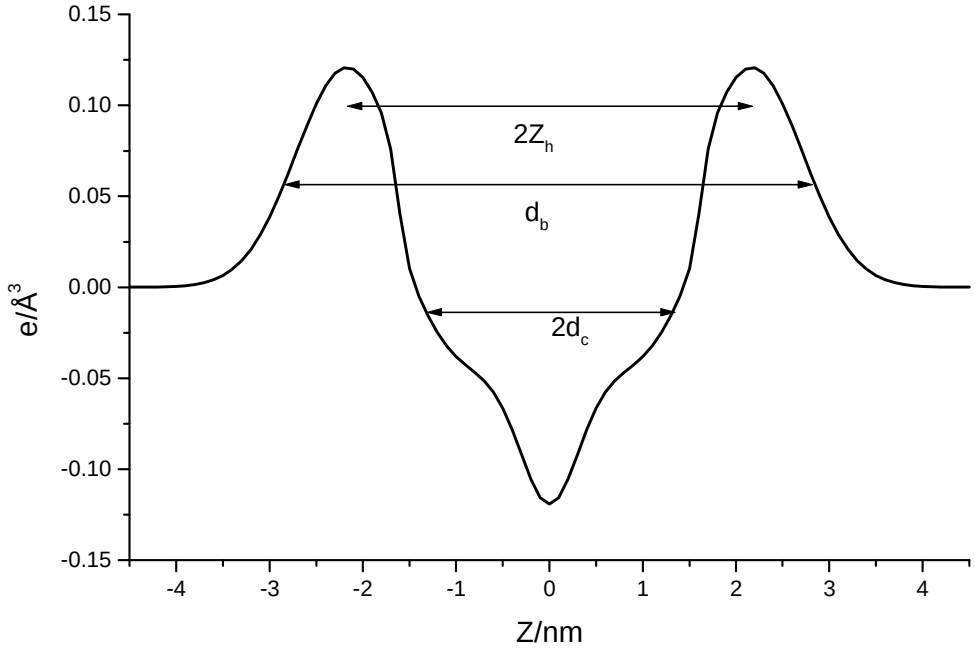

Figure S1. Electronic density profile showing some of the S